Chinese Chemical Letters 35 (2024) 108824

Contents lists available at ScienceDirect

Chinese Chemical Letters

journal homepage: www.elsevier.com/locate/cclet

The remarkable effect of amino hydrogen on membrane permeability and organelle staining of 1,8-naphthalimide dyes

Zhifeng Li[a,b], Qinglong Qiao[b,*], Ning Xu[a,b], Kai An[b,c], Wenchao Jiang[b,c], Yi Tao[b,c], Pengjun Bao[b,c], Yinchan Zhang[b,c], Zhaochao Xu[a,b,*]

[a] School of Chemistry, Dalian University of Technology, Dalian 116024, China
[b] CAS Key Laboratory of Separation Science for Analytical Chemistry, Dalian Institute of Chemical Physics, Chinese Academy of Sciences, Dalian 116023, China
[c] University of Chinese Academy of Sciences, Beijing 100049, China

ARTICLE INFO

Article history:
Received 14 June 2023
Revised 17 July 2023
Accepted 18 July 2023
Available online 20 July 2023

Keywords:
Amino hydrogen
1,8-Naphthalimide
Cell permeability
Lipid droplet
Lysosome

ABSTRACT

Membrane permeability and intracellular diffusion of fluorescent probes determine staining selectivity of intracellular substructures. However, the relationship between the molecular structure of fluorescent probes and their membrane permeability and intracellular distribution is poorly understood. In this paper, we reported a series of 1,8-naphthalimide dyes and carried out cell imaging experiments, and found that the presence of amino hydrogen in these dyes played a crucial role in their cell membrane permeability and intracellular distribution. The secondary amino group containing compounds **1**–**4** show excellent membrane permeability and strong fluorescence in living cells. While the tertiary amine containing dyes **5** and **6** can hardly permeate the cell membrane though they show extremely similar structure with compounds **2**–**4**. Compound **1** can selectively image lipid droplets by selecting the wavelength of excitation light. With the specificity for lysosomes, **2** and **4** have been used in long-term time-lapses imaging of lysosomal dynamics and tracking the process of lysosome–lysosome interaction, fusion and movement. The effect of hydrogen-containing amino substituent on the cell membrane permeability of fluorescent molecules is promising for the development of better biocompatible probes.

The demand for visualization of physiological and pathological mechanisms in life sciences has driven the rapid development of fluorescent probes from their birth to the present [1,2]. This "receptor-linker-fluorophore" probe relies on the environmental sensitivity of fluorescent dyes to light the target [3,4]. The working principle has been used since the realization of calcium ion recognition and imaging in living cells [5,6]. In recent years, super-resolution fluorescence imaging, which relies on the time resolution of fluorescence to break through the diffraction limit, has injected new vitality into the research of dye chemistry [7–10]. In order to meet the requirements of single-molecule imaging in terms of spatiotemporal resolution, fluorescence brightness and stability [11], after the rise of antibody fluorescent labeling [12] and *in vivo* imaging such as fluorescence-guided surgery [13], a new wave of research on traditional dyes such as rhodamine and cyanine has been launched [14–17]. The new focus is on developing new synthetic methods [18,19], discovering new fluorophores [20–22], studying the molecular mechanism of photobleaching [23,24], regulating the target recognition selectivity of fluorescent probes through reversible covalent bonding reactions [25–27], *etc*. As exogenous molecules, fluorescent probes must have good cell membrane penetration, directional transport in cells, rapid identification and labeling after finding the target [28,29]. These are important factors that affect the quality of biological imaging. As fluorescence imaging enters the level of single-molecule, how to make fluorescent probes have good membrane permeability and how to guide their transport in cells has become an urgent problem to be solved.

There are mainly two empirical methods for endowing fluorescent probes with intracellular targeting capabilities. The most widely used method is to introduce molecular recognition groups on fluorescent dyes to achieve binding to target molecules [30–33], such as relying on the interaction of antibodies and antigens, genetically encoded tags that catalyze coupling between enzyme-substrates, bioorthogonal reaction pairs, or small molecules capable of non-covalently active binding to biomacromolecules. With this approach, the imaging of different organelles and the detection of active species within the organelles became possible. Currently widely recognized localization dyes include, cationic dyes that selectively stain the mitochondrial inner membrane through

* Corresponding authors.
E-mail addresses: qqlqiao@dicp.ac.cn (Q. Qiao), zcxu@dicp.ac.cn (Z. Xu).

https://doi.org/10.1016/j.cclet.2023.108824
1001-8417/

electrostatic attraction [34,35], and dyes that are linked to substrate molecules are covalently linked to SNAP-tag and Halo-tag to label fusion organelle structural proteins [36,37], thereby realizing labeling of different organelles, *etc*. However, this method of introducing empirical localization groups often faces the problem that the designed fluorescent probes do not have a predetermined intracellular localization or membrane permeability, which is probably due to the specific intracellular localization of the dye itself or the binding of non-target molecules.

Another approach is to build a diversity-oriented fluorescent dye library to screen out probes with specific functions [38]. This method does not require the modification of cells by genetic coding, ensuring the originality of cells, but it requires the synthesis of a large number of dye molecules. How to ensure the diversity of dye structures and systematically analyze the environmental sensitivity of dyes with different structures is the key to discovering dyes with specific targeting in cells. When understanding the intracellular targeting of fluorescent probes screened by diversity-oriented methods, more attention is paid to dyes' size, three-dimensional configuration and lipophilicity. Although the key role of specific structural components of drugs has been demonstrated in medicinal chemistry, for the development of fluorescent probes with membrane permeability and intracellular localization, the discovery and reporting of key structural components that determine these properties are still very lacking [39]. Structural components in dyes have been focused more on their effects on fluorescent properties than on the fate of dyes in cells.

In this paper, we reported that the secondary amino substitute connected to 1,8-naphthalimide dyes has a critical impact on their membrane permeability and intracellular localization (Scheme 1). Compound **1** is a typical 1,8-naphthalimide dye conjugated with a secondary amino group to ensure high fluorescence brightness. For compounds **2**–**6**, a second amino group attached to the fluorophore through the ethylene group will quench the fluorescence through the photo-induced electron transfer (PET) process, thus becoming acid-sensitive probes. In compounds **3**–**6**, the tertiary amine conjugated with the chromophore also has the twisted intramolecular charge transfer (TICT) effect to synergistically quench the fluorescence intensity. It is found that dyes where amine groups containing hydrogen atoms were membrane-permeable, while dyes where amine groups without hydrogen atoms were difficult to permeate the cell membrane. Then, only compounds **2**–**4** could selectively stain lysosomes and track the lysosomal dynamics including lysosome-lysosome contact and fusion with fluorescent imaging.

The absorption and fluorescence spectra of the six naphthalimide dyes in different solvents were firstly examined (Fig. S1 in Supporting information and Table 1). As expected, compound **1** showed an obvious red shift from 502 nm in $CHCl_3$ to 554 nm in water, showing high sensitivity to solvent polarity (Fig. S1). Furthermore, the quantum yield (φ) of compound **1** in organic solvents were all above 0.6 (Table 1). Compounds **2**–**6** showed less sensitivity to solvent polarity, and their emission wavelengths in water were all around 530 nm which exhibited significant blue shift compared with compound **1**. This blue shift in emission was ascribed to the protonation of remote N atom and the associated intramolecular hydrogen bond decreased the electron donating capability of the conjugated N atom in the 4-position of 1,8-naphthalimide. Their quantum yields in water were much higher than those in polar solvents due to the inhibition of PET by protonation, especially for compounds **2**, **3** and **6**. However, due to the strong TICT effect, the quantum yields of compounds **4** and **5** in water were below 0.03. In compounds **3** and **6**, it was also believed that there was a TICT effect to quench the fluorescence, but their quantum yields in water were 0.18 and 0.49, respectively. This was most likely due to the protonation and formed intramolecular hydrogen bond enhanced the rigidity of piperazine and simultaneously suppressed TICT. It was also worth noting that compounds **2**–**4**, where amine groups containing hydrogen atoms, showed considerable quantum yields in $CHCl_3$ compared with compounds **5** and **6** where amine groups containing no hydrogen atoms. It can be seen from the above data that the presence of amino hydrogen has a significant effect on the fluorescence intensity and wavelength of these dyes in different environments. The presence of amino hydrogen also affects the cell permeability and intracellular staining properties of these dyes.

To further examine the effect of protonation on emission, their fluorescence responses to different pH ranging from 2.0 to 12.0 were next investigated (Fig. 1 and Fig. S2 in Supporting information). With the increase of pH value, the fluorescence intensity of compounds **2**–**6** all increased significantly and showed a negative correlation with pH value (Fig. S2). This was because the pH sensitive moiety showed high PET efficient in alkaline environment due to the electron transfer from amine to 1,8-naphthalimide flu-

Table 1
Optical properties of compounds **1**–**6** in various solvents.

Dye	Solvent	λ_{abs} (nm)	λ_{em} (nm)	ε (L mol^{-1} cm^{-1})	$\Delta\lambda$ (nm)	φ
1	$CHCl_3$	428	502	14,049	74	0.832
	ACN	431	518	14,839	87	0.629
	EtOH	443	529	16,202	86	0.652
	DMSO	444	526	14,856	82	0.805
	H_2O	450	554	11,936	104	0.099
2	$CHCl_3$	430	500	17,186	70	0.762
	ACN	430	520	17,595	90	0.018
	EtOH	437	519	17,575	82	0.029
	DMSO	444	531	17,135	87	0.013
	H_2O	433	531	16,440	98	0.387
3	$CHCl_3$	400	509	10,378	109	0.142
	ACN	403	512	9381	109	0.012
	EtOH	400	507	9203	107	0.027
	DMSO	405	517	10,561	112	0.063
	H_2O	392	533	9819	141	0.180
4	$CHCl_3$	405	496	9804	91	0.551
	ACN	412	506	10,188	94	0.257
	EtOH	408	513	9808	105	0.114
	DMSO	419	520	9296	101	0.078
	H_2O	401	534	9372	133	0.029
5	$CHCl_3$	412	500	11,849	88	0.026
	ACN	418	509	11,369	91	0.020
	EtOH	414	511	11,210	97	0.006
	DMSO	428	516	11,285	88	0.003
	H_2O	403	534	10,583	131	0.013
6	$CHCl_3$	399	504	11,087	105	0.076
	ACN	400	515	10,481	115	0.005
	EtOH	398	521	10,331	123	0.012
	DMSO	407	516	9849	109	0.020
	H_2O	390	528	9797	138	0.492

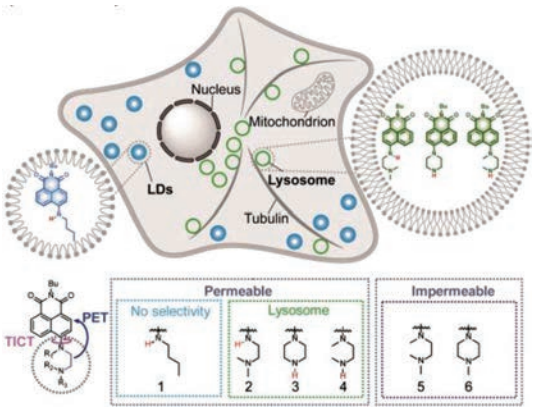

Scheme 1. Structures of compounds **1**–**6** and their cellular permeability.

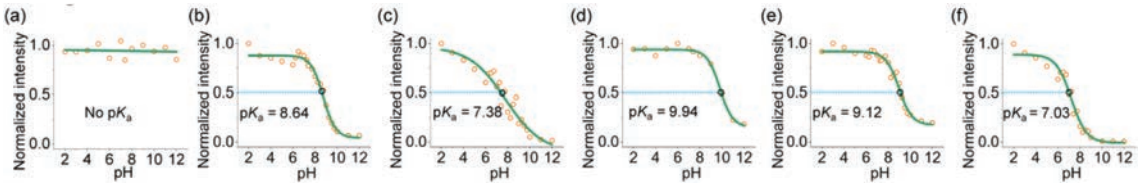

Fig. 1. Normalized intensity of compounds **1–6** as a function of pH in aqueous solution. (a) **1**; (b) **2**; (c) **3**; (d) **4**; (e) **5**; (f) **6**.

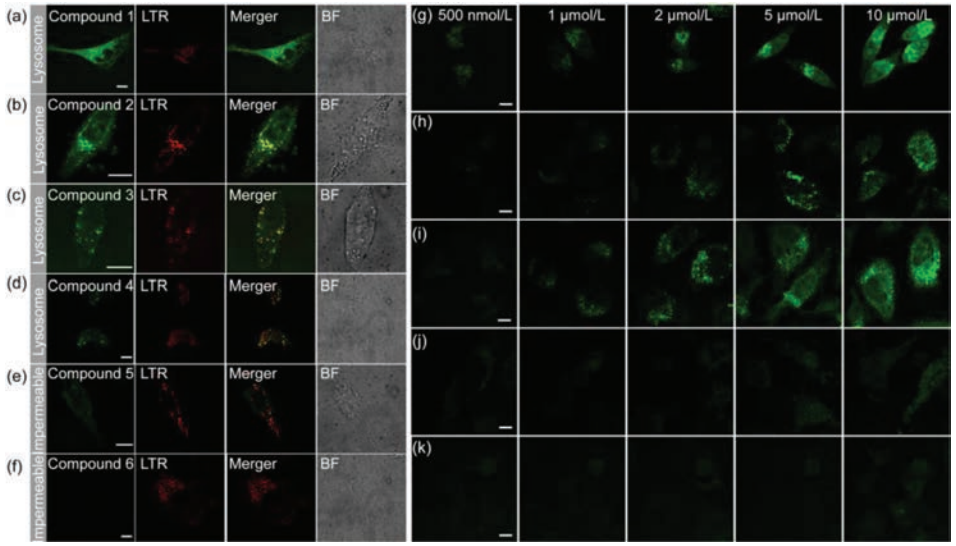

Fig. 2. (a–f) Confocal images of living HeLa cells using different concentrations of compounds **1–6** and co-localized with imaging with commercial available organelle indicators. LTR is the abbreviation of Lyso-Tracker Red. (g–k) Confocal images of HeLa cells using different concentrations of compounds **2–6**. Scale bar = 10 μm.

orophore, resulting in non-fluorescence state. Once the remote N atom was protonated, PET would be inhibited to recover the fluorescence. The absorption spectra of compounds **2–6** exhibited obvious blue shift with the decrease of pH value, also confirming that the associated intramolecular hydrogen bond after protonation decreased the electron donating capability of the conjugated N atom in the 4-position of 1,8-naphthalimide.

The fluorescence intensities of compounds **2–6** at pH 2 were enhanced 15.1, 63.4, 4.8, 4.7, 123.3 folds compared with that at pH 12, respectively (Fig. S3 in Supporting information). For compounds **3** and **6**, more than 60-fold fluorescence enhancement after protonation was not only due to the inhibition of PET, but also due to the inhibition of TICT (Table S1 in Supporting information). The thorough protonation of piperazine derivatives suppressed TICT and enabled the quantum yield of dyes **3** and **6** to reach 0.51 and 0.74 at pH 2. However, because of the formation of rigid piperazine salt, the pK_a of compounds **3** and **6** were only 7.38 and 7.03 (Fig. 1), respectively, which were much lower than that of other three dyes. The pK_a values of **2**, **4** and **5** were 8.64, 9.94 and 9.12, respectively. Although compounds **4** and **5** were highly sensitive to pH, the strong TICT effect made their quantum yields less than 0.024 at pH 2. Remarkably, the N–H containing dye **4** showed higher quantum yield than dye **5** which had no N–H. The same results were found between compounds **3** and **6**. These results indicated that the secondary amine had lower PET efficiency than the tertiary amine.

The performances in live-cell fluorescence imaging were next performed through directly incubating HeLa cells with these dyes (Fig. 2). The N–H containing dyes **1–4** could permeate cell membrane and display high fluorescence at specific cellular locations. Whereas the cells incubated with dyes **5** and **6** without N–H group showed negligible cellular fluorescence, indicating that these two dyes were difficult to enter the cell. It was observed that compound **1** could stain multiple organelles. Based on the co-localization imaging with commercial available organelle dyes including Mito-Tracker Orange, Lyso-Tracker Red and LD-Tracker Deep Red, dye **1** was found to simultaneously stain mitochondria, lysosomes and lipid droplets (Fig. 2a and Fig. S5 in Supporting information). When changing the 488 nm excitation light to a 405 nm laser, only lipid droplets can be fluorescently imaged (Fig. S5c). Compounds **2** and **4** located in lysosomes with high specificity, showing co-localization with Lyso-Tracker Red. The intensity profiles of the linear regions across HeLa cells in Fig. S6 (Supporting information) were in close synchrony, further confirming their high location accuracy to lysosomes. We attributed the lysosome specificity to their lysosomal pH sensitive fluorogenicity. Although compounds **5** and **6** had similar pH sensitive ranges to compounds **2–4**, and even compound **5** has 0.50 quantum yield at lysosomal pH, they could not enter living cells and light up lysosomes. We therefore speculated that the amino hydrogen in these six 1,8-naphthalimide dyes might serve as a trigger to modulate their permeability to living cells and cellular localization.

To examine their permeability in detail, we incubated live HeLa cells at 37 °C using different concentration of these dyes (Fig. 2). Compounds **2–4** could clearly image lysosomes at 500 nmol/L and maintain high specificity for lysosomes below 2.0 μmol/L. The cells also showed enhanced lysosomal fluorescence with increasing dye concentrations (Figs. 2g–i). Once the incubation concentration of dyes exceeded 5.0 μmol/L, excess dyes would locate in nucleus due to the weaker affinity to DNA. The cells incubated with compounds **5** and **6** remained dark throughout despite the dye concentrations were as high as 10.0 μmol/L (Figs. 2j and k). These results further confirmed that the N–H in 1,8-naphthalimide dyes indeed could enable them to permeate the cell membranes.

Due to the excellent specificity for lysosomes and high quantum yield at lysosomal pH, the dynamic of lysosomes was tracked with

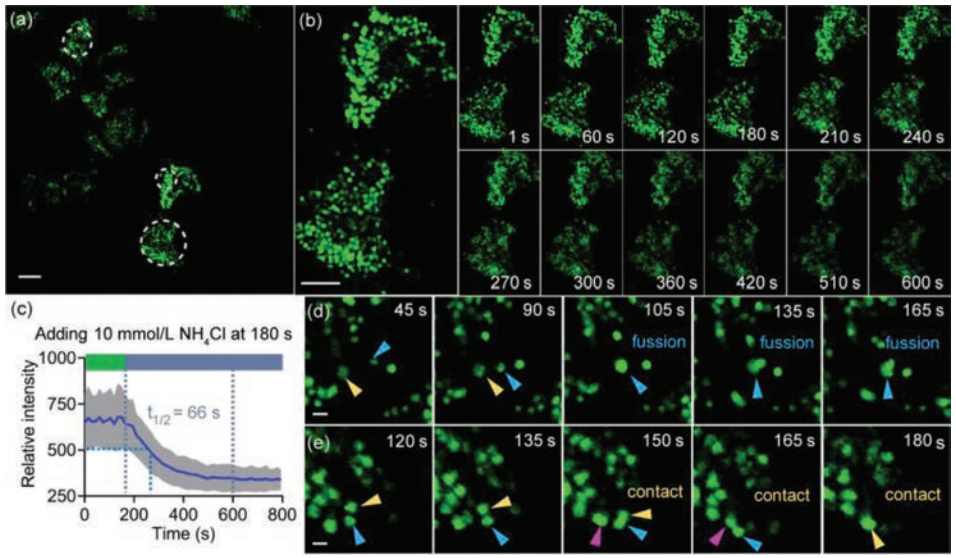

Fig. 3. (a, b, d, e) Confocal imaging of lysosomes in living HeLa cells which were incubated with 1 μmol/L compound **2** for 30 min. Excited with 488 nm laser, collected: 500–600 nm. (b, d, e) Imaging of the lysosomal dynamics in live HeLa cells. (c) Curves of fluorescence intensity changes with time in (a). The imaging interval was 15 s. $t_{1/2} = 66$ s. (a, b) Scale bar: 10 μm. (d, e) Scale bar: 1.0 μm.

compound **2** (Fig. 3). Intracellular alkalization was first performed by adding 10 mmol/L NH_4Cl to living cells in order to simulate alkalosis (Figs. 3a and b). A nearly 46% decrease in lysosomal fluorescence intensity was observed after the addition of NH_4Cl after 180 s (Fig. 3c). And the whole alkalization of lysosomes was a prolonged process lasting more than 7 min, and compound **2** displayed a quick response speed with a $t_{1/2}$ of 66 s. In addition, compound **4** was also able to monitor lysosomal pH, although it showed slower response speed compared to compound **2** (Figs. S7a–c in Supporting information). Through the long-term time-lapse imaging, we also monitored diverse lysosomal dynamic including lysosome-lysosome fusion and short contact. As shown in Fig. 3d, a rapid lysosome fusion was observed. The lysosome marked by blue arrow in Fig. 3d showed highly dynamic and moved towards the motionless lysosome labelled by yellow arrow. At 105 s, the two isolated lysosomes fused to form a new lysosome which continuously changed morphology during 105–165 s. Furthermore, the rapid contact between two isolated lysosomes was observed at 150 s and 180 s in Fig. 3e. More lysosome–lysosome contacts were also imaged using compound **4**, indicating that the hydrogen in the amine groups could certainly endow the 1,8-naphthalimide dyes high permeability and excellent lysosome selectivity.

In summary, we synthesized a series of amino-substituted 1,8-naphthalimide dyes and revealed that the amino-hydrogen (N–H) served as a trigger to modulate their permeability to living cells. The N–H containing dyes **2**–**4** showed high membrane permeability, while compounds **5** and **6** with no N–H were almost impermeable to cell membrane. Furthermore, the PET and TICT mechanisms could synergistically regulate the emission of these dyes and endow them with environmental sensitivity to pH and excellent specificity to lysosomes and lipid droplets. Compound **1** can selectively image lipid droplets, and compounds **2** and **4** could rapidly permeate cell membrane and stain lysosomes, allowing long-term time-lapses imaging to record lysosomal dynamics including fusion, contact and motion. As the cells were alkalized, we could also monitor pH changes through a decrease in lysosomal fluorescence intensity. It is worth noting that rational introduction of active amino hydrogen into organic fluorophores can not only regulate fluorescence properties, but also affect the fate of dyes in cells, thus prompting us to develop diverse fluorescence probes with better biocompatibility.

Declaration of competing interest

The authors declare that they have no known competing financial interests or personal relationships that could have appeared to influence the work reported in this paper.

Acknowledgments

This work is supported by the National Natural Science Foundation of China (Nos. 22278394, 22078314 and 21908216) and Dalian Institute of Chemical Physics (Nos. DICPI202227 and DICPI202142).

Supplementary materials

Supplementary material associated with this article can be found, in the online version, at doi:10.1016/j.cclet.2023.108824.

References

[1] J. Zhang, R.E. Campbell, A.Y. Ting, R.Y. Tsien, Nat. Rev. Mol. Cell Biol. 3 (2002) 906–918.
[2] W.J. Liu, J. Chen, Z.C. Xu, Coord. Chem. Rev. 429 (2021) 213615.
[3] Z. Xu, J. Yoon, D.R. Spring, Chem. Soc. Rev. 39 (2010) 1996–2006.
[4] W.W. Liu, L. Miao, X.L. Li, Z.C. Xu, Coord. Chem. Rev. 429 (2021) 213646.
[5] G. Grynkiewicz, M. Poenie, R.Y. Tsien, J. Biol. Chem. 260 (1985) 3440–3450.
[6] J. Pan, W. Lin, F. Bao, et al., Chin. Chem. Lett. 34 (2023) 107519.
[7] J. Chen, C. Wang, W. Liu, et al., Angew. Chem. Int. Ed. 60 (2021) 25104–25113.
[8] J.B. Grimm, L.D. Lavis, Nat. Methods 19 (2022) 149–158.
[9] Q. Qiao, W. Liu, J. Chen, et al., Angew. Chem. Int. Ed. 61 (2022) e202202961.
[10] Q. Qiao, W. Liu, Y. Zhang, et al., Angew. Chem. Int. Ed. 61 (2022) e202208678.
[11] M. Fernandez-Suarez, A.Y. Ting, Nat. Rev. Mol. Cell Biol. 9 (2008) 929–943.
[12] A.H. Coons, H.J. Creech, R.N. Jones, E. Berliner, J. Immunol. 45 (1942) 159–170.
[13] Q.T. Nguyen, E.S. Olson, T.A. Aguilera, et al., Proc. Natl. Acad. Sci. U. S. A. 107 (2010) 4317–4322.
[14] G.T. Dempsey, M. Bates, W.E. Kowtoniuk, et al., J. Am. Chem. Soc. 131 (2009) 18192–18193.
[15] C. Wang, W. Chi, Q. Qiao, et al., Chem. Soc. Rev. 50 (2021) 12656–12678.
[16] W. Zhou, X. Fang, Q. Qiao, et al., Chin. Chem. Lett. 32 (2021) 943–946.
[17] H. Fukushima, S.S. Matikonda, S.M. Usama, et al., J. Am. Chem. Soc. 144 (2022) 11075–11080.
[18] F. Deng, L. Liu, W. Huang, et al., Spectrochim. Acta A Mol. Biomol. Spectrosc. 240 (2020) 118466.
[19] J.B. Grimm, T.A. Brown, A.N. Tkachuk, L.D. Lavis, ACS Cent. Sci. 3 (2017) 975–985.
[20] M. Fu, Y. Xiao, X. Qian, et al., Chem. Commun. (2008) 1780–1782.
[21] T. Egawa, K. Hanaoka, Y. Koide, et al., J. Am. Chem. Soc. 133 (2011) 14157–14159.
[22] M.S. Michie, R. Gotz, C. Franke, et al., J. Am. Chem. Soc. 139 (2017) 12406–12409.

[23] Q. Zheng, M.F. Juette, S. Jockusch, et al., Chem. Soc. Rev. 43 (2014) 1044–1056.
[24] Y. Ji, W. Mu, H. Wu, Y. Qiao, Adv. Sci. 8 (2021) 2101187.
[25] Q. Qi, W. Chi, Y. Li, et al., Chem. Sci. 10 (2019) 4914–4922.
[26] W. Chi, Q. Qiao, C. Wang, et al., Angew. Chem. Int. Ed. 59 (2020) 20215–20223.
[27] Y. Zhang, W. Zhou, N. Xu, et al., Chin. Chem. Lett. 34 (2023) 107472.
[28] L. Miao, C. Yan, Y. Chen, et al., Cell Chem. Biol. 30 (2023) 248–260.
[29] W. Zhou, Q.L. Qiao, Y. Tao, et al., Sens. Actuator. B: Chem. 376 (2023) 132980.
[30] W. Xu, Z. Zeng, J.H. Jiang, et al., Angew. Chem. Int. Ed. 55 (2016) 13658–13699.
[31] J. Chen, W. Liu, X. Fang, et al., Chin. Chem. Lett. 33 (2022) 5042–5046.
[32] W. Liu, J. Chen, Q. Qiao, et al., Chin. Chem. Lett. 33 (2022) 4943–4947.
[33] Q. Qiao, W. Liu, W. Chi, et al., Aggregate 4 (2022) e258.
[34] T.X. Jin, M.Y. Cui, D. Wu, et al., Chin. Chem. Lett. 32 (2021) 3899–3902.
[35] B.B. Wang, X.Q. Wang, A.Q. Zeng, et al., Sens. Actuator. B: Chem. 343 (2021) 130095.
[36] W.J. Liu, Q.L. Qiao, J.Z. Zheng, et al., Biosens. Bioelectron. 176 (2021) 112886.
[37] J. Li, Q.L. Qiao, Y.Y. Ruan, et al., Chin. Chem. Lett. 34 (2023) 108266.
[38] S.W. Yun, N.Y. Kang, S.J. Park, et al., Acc. Chem. Res. 47 (2014) 1277–1286.
[39] H. Ungati, V. Govindaraj, G. Mugesh, Angew. Chem. Int. Ed. 57 (2018) 8989–8993.